

## Article

# Use of Biochar-Based Cathodes and Increase in the Electron Flow by *Pseudomonas aeruginosa* to Improve Waste Treatment in Microbial Fuel Cells

Rosa Anna Nastro <sup>1,\*</sup>, Fabio Flagiello <sup>2</sup>, Nicandro Silvestri <sup>3</sup>, Edvige Gambino <sup>4</sup>, Giacomo Falcucci <sup>5,6,\*</sup>   
and Kuppam Chandrasekhar <sup>7</sup>

<sup>1</sup> EN-TECH ITALIA srl, Gragnano, 80054 Naples, Italy

<sup>2</sup> Department of Engineering, University Parthenope of Naples—Centro Direzionale Isola C4, 80133 Naples, Italy; flagiellofabio@gmail.com

<sup>3</sup> ING Silvestri Consulting, 86079 Venafro, Italy; nicandrosilvestri@gmail.com

<sup>4</sup> Department of Biology, University of Naples “Federico II”, 80126 Naples, Italy; ed.gambino@gmail.com

<sup>5</sup> Department of Enterprise Engineering “Mario Lucertini”, University of Rome “Tor Vergata”, 00133 Rome, Italy

<sup>6</sup> Department of Physics, Harvard University, Cambridge, MA 02138, USA

<sup>7</sup> Department of Biotechnology, National Institute of Technology Warangal, Telangana 506004, India; chanduibt@gmail.com

\* Correspondence: rosa.nastro@collaboratore.uniparthenope.it (R.A.N.); giacomo.falcucci@uniroma2.it (G.F.)



**Citation:** Nastro, R.A.; Flagiello, F.; Silvestri, N.; Gambino, E.; Falcucci, G.; Chandrasekhar, K. Use of Biochar-Based Cathodes and Increase in the Electron Flow by *Pseudomonas aeruginosa* to Improve Waste Treatment in Microbial Fuel Cells. *Processes* **2021**, *9*, 1941. <https://doi.org/10.3390/pr9111941>

Academic Editor: Domenico Frattini

Received: 21 August 2021

Accepted: 25 October 2021

Published: 29 October 2021

**Publisher’s Note:** MDPI stays neutral with regard to jurisdictional claims in published maps and institutional affiliations.



**Copyright:** © 2021 by the authors. Licensee MDPI, Basel, Switzerland. This article is an open access article distributed under the terms and conditions of the Creative Commons Attribution (CC BY) license (<https://creativecommons.org/licenses/by/4.0/>).

**Abstract:** In this paper, we tested the combined use of a biochar-based material at the cathode and of *Pseudomonas aeruginosa* strain in a single chamber, air cathode microbial fuel cells (MFCs) fed with a mix of shredded vegetable and phosphate buffer solution (PBS) in a 30% solid/liquid ratio. As a control system, we set up and tested MFCs provided with a composite cathode made up of a nickel mesh current collector, activated carbon and a single porous poly tetra fluoro ethylene (PTFE) diffusion layer. At the end of the experiments, we compared the performance of the two systems, in the presence and absence of *P. aeruginosa*, in terms of electric outputs. We also explored the potential reutilization of cathodes. Unlike composite material, biochar showed a life span of up to 3 cycles of 15 days each, with a pH of the feedstock kept in a range of neutrality. In order to relate the electric performance to the amount of solid substrates used as source of carbon and energy, besides of cathode surface, we referred power density (PD) and current density (CD) to kg of biomass used. The maximum outputs obtained when using the sole microflora were, on average, respectively  $0.19 \text{ Wm}^{-2}\text{kg}^{-1}$  and  $2.67 \text{ Wm}^{-2}\text{kg}^{-1}$ , with peaks of  $0.32 \text{ Wm}^{-2}\text{kg}^{-1}$  and  $4.87 \text{ Wm}^{-2}\text{kg}^{-1}$  of cathode surface and mass of treated biomass in MFCs with biochar and PTFE cathodes respectively. As to current outputs, the maximum values were  $7.5 \text{ Am}^{-2} \text{ kg}^{-1}$  and  $35.6 \text{ Am}^{-2}\text{kg}^{-1}$  in MFCs with biochar-based material and a composite cathode. If compared to the utilization of the sole acidogenic/acetogenic microflora in vegetable residues, we observed an increment of the power outputs of about 16.5 folds in both systems when we added *P. aeruginosa* to the shredded vegetables. Even though the MFCs with PTFE-cathode achieved the highest performance in terms of PD and CD, they underwent a fouling episode after about 10 days of operation, with a dramatic decrease in pH and both PD and CD. Our results confirm the potentialities of the utilization of biochar-based materials in waste treatment and bioenergy production.

**Keywords:** waste-to-energy systems; solid organic waste treatment; microbial fuel cells; *Pseudomonas aeruginosa*; biochar

## 1. Introduction

Bioenergy is a promising and feasible alternative to fossil fuels and a sustainable waste management solution. The scientific community is now working hard to discover and develop low-cost materials that may substantially enhance the performance of microbial

fuel cells (MFCs) and expand their applications in waste and wastewater treatment [1–9]. The interest in MFCs and, more in general, in bioelectrochemical systems (BESs), lies in the possibility to join waste treatment and energy recovery with commodity chemical production by electrosynthesis processes [10–13]. Briefly, electrosynthesis relies on the utilization of electrons produced by electroactive bacteria (or provided by an external source) to drive microbial metabolism towards the biosynthesis of chemicals such as H<sub>2</sub>, fatty acids, methane and other chemicals. A process strictly related to electrosynthesis is electrofermentation [10–18]. All the above-mentioned processes are indeed promising and are able to contribute to the transition to the circular economy and sustainable development [2,19–21].

### 1.1. Biochar: A Promising Electrode Material

Many studies have recently shown the applicability of biochars as anodes, cathodes, and semipermeable membrane materials in MFCs [7,22–27]. Biochars are complex, heterogeneous materials consisting of mineral phases, amorphous carbon, graphitic carbon, and labile organic molecules, many of which can be either electron donors or acceptors [7,24]. Joseph et al. reported in [28] that nanoparticles with redox-active Fe- and Mn-based minerals, usually present in high-temperature biochars, play an important role in mediating the direct electronic transfer (DET) among bacteria (such as *Geobacter* spp and *Shewanella oneidensis*) and the anode. Other properties at the basis of the utilization of biochars, such as anode materials, are the high specific surface, its biocompatibility and resistance to corrosion, the high electrical conductivity, low ohmic resistance, chemical stability and hydrophilicity [27]. As we previously reported, biochar can also act as a cathode, mainly due to the presence of heteroatoms characterized by charge delocalization, reduced charge transfer resistance and low activation energy barrier, besides high stability and specific surface [27]. Thanks to its electrochemical properties and low cost, biochar has been identified as a good candidate material to be used in the set-up of scaled BESs for wastewater treatment and soil bioremediation [7,23,27,29]. A benefit of biochar, in comparison to other carbon-based materials, such as activated carbon (AC), lies in its easy production from different vegetable residues and from sewage sludge [7,13,22,27,30–32]. Finally, different researches have proved biochar-based materials to be suitable also for dye degradation, landfill leachate, and other pollutants treatment in MFCs, which adds a further benefit to the ones described above [27,33,34].

### 1.2. MFCs and Solid Organic Residues

Different researchers have proven the reliable utilization of MFC technology to the treatment and valorization of organic residues [5,16,20,26,35–37].

Compared to anaerobic digestion (AD), MFCs can achieve a higher chemical oxygen demand (COD) removal, with a consistent reduction of energy consumption and avoiding net CO<sub>2</sub> emissions. Moreover, the use of MFCs as a biomass pre-treatment enhances biohydrogen production by dark fermentation [11,18], with energy recovery in terms of current and power outputs [38].

One of the disadvantages related to the direct use of solid residues in MFCs lies in the competition between fermentative microflora, usually present in organic residues, and electroactive bacteria [5,19,35,36]. Besides such a competition, the resistance opposed by solid particles to the electrons and cation flow affects the performance of MFCs fed with solid organic substrates [5,9]. Furthermore, pH drops can occur in consequence of lactic-acid fermentation prevailing over other metabolic pathways [5,9,16,39]. Such factors put electrodes materials on the test as they are much more exposed to fouling if compared to MFC fed with municipal wastewater [37].

### 1.3. Principle of Electron Transfer

The ability of electroactive biofilms to exchange electrons with the electrodes is at the basis of power generation in MFCs. Bacteria may use different ways to drive the electrons to an anode: with direct exchange (usually via cytochromes or, more in general, oxydore-

ductases), by electron shuttles, i.e., inorganic compounds like  $\text{Fe}^{3+}$  or  $\text{Mn}^{4+}$  or organic molecules, like flavins and phenazines, able to undergo to a reversible oxidation/reduction reaction [40]. Some microbial species like *Shewanella oneidensis* and *Geobacter sulfurreducens* use nanowires, i.e., long filaments originating from the cell membrane acting as “nanoleads” to transfer electrons directly from the cell to the electrode [40]. It has been noticed that “not shuttle producers” like a great part of Gram-positive bacteria can take advantage of such compounds produced by other microbial species, thus increasing the number of electrons transferred to the anode, with substantial metabolic advantages (Figure 1) [41,42].

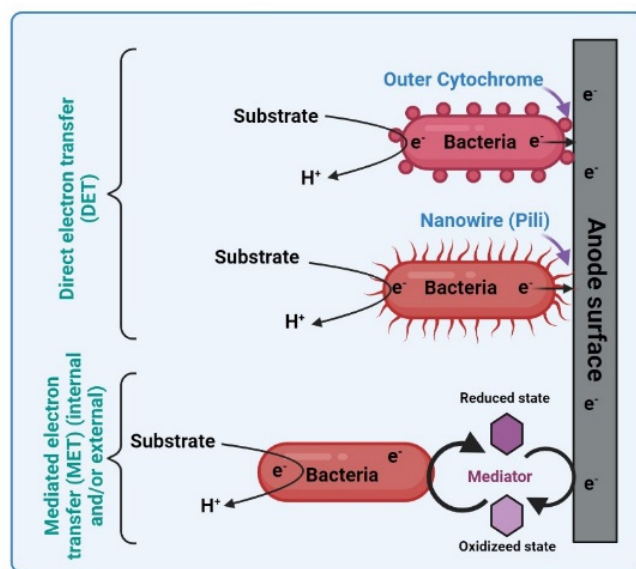


**Figure 1.** Mechanisms of direct electron transfer (DET) and mediated electron transfer (MET). Potential interactions between shuttle producers and no producer bacteria in an electroactive biofilm can occur as no producers can use such molecules as mediators to deliver  $e^-$  to the anode. No producers transfer electrons directly to the anode.

In [43], the authors report how supernatants of a *Pseudomonas chlororaphis* PCL1121 producing phenazine-1-carboxamide enhanced the electricity generation in an MFC inoculated with a mixed culture. Since then, many researchers have demonstrated not only the enhancement of BESs performance in the presence of mediators at the anode but also the ability of biofilms to store a certain amount of molecules that can act as both intracellular electron acceptors and shuttles to the electrode [40,42].

#### 1.4. Acidogenic and Acetogenic Microflora in Organic Waste

*Bacillaceae*, *Lactobacillaceae*, *Clostridiaceae*, *Enterobacillaceae*, *Streptococcaceae* are the main components of the microflora colonizing vegetable fresh residues, besides *Pseudomonadaceae* and some *Enterobacteriaceae*. Most of them are in great part characterized by a fermentative metabolism. Among them, acidogenic and acetogenic microorganisms play an important role in anaerobic digestion and dark fermentation [35,44,45]. Most parts of such microorganisms are listed among weakly or not electroactive bacteria. As they mostly use direct electron transfer and/or have defective electron transport chains, they are less effective in producing electric power in MFCs if compared to Gram-negative, non-fermentative bacteria [46]. As an example, *Lactobacillaceae* are widely colonizing vegetable residues and are characterized by an incomplete electron transport chain, involved in nitrate reduction and in the respiration-like behavior under aerobic conditions [47]. Even so, an increasing number of papers have reported extracellular electron transfer, and the exchange of electrons with an electrode in Gram-positive, fermentative bacteria [11,35,46]. The utilization of a proper inoculum, enriched in bacteria able to produce electron car-

ries, can lead to an improvement of the electron flow from the biofilm to the anode, thus improving current and power outputs.

### 1.5. Aim of the Research

In this paper, we present the results of a survey aimed at assessing the potential utilization of *Pinus resinosa* wood biochar bars to create cathodes in MFCs (B-MFCs) fed with organic solid residues. We used, as control systems, MFCs with the same layout but provided with a cathode made up of a nickel-mesh collector, activated-carbon layer, and a porous PTFE diffusion layer (P\_MFC) (VITO©, Boeretang, Belgium). Furthermore, we investigated the effect of the addition of a *Pseudomonas aeruginosa* ATCC 15,692 strain to the microflora naturally occurring in the organic residues, mainly composed by *Lactobacillaceae* and *Bacillaceae* on MFCs performance.

## 2. Materials and Methods

### 2.1. Biochar-Based Cathode Constructing and Testing

We produced biochar material from *Pinus resinosa* wood by means of a high-temperature pyrolysis (850 °C) able to increase the surface area and carbonized fractions (graphite-like structures), decrease the cation exchange capacity and increase the ability to exchange electrons [48,49]. An industrial press at 700 ton/cm<sup>2</sup> compressed the obtained biochar to obtain bars of 5 cm width, 6 cm height, and 4 cm depth. We further exposed the bars to high temperatures (1000–1200 °C) during a blast furnaces operation and, eventually, cut into slices of 0.4 cm thickness and then used them in membrane-less MFCs as air-breathing cathodes, after rinsing them with distilled water. Before using them, we measured biochar effective porosity  $\phi$  (volume of space connected to the outer surface of the solid) and density  $d$  according to the following formulas:

$$\phi = \left( \frac{Vv}{Vs} \right) * 100 \quad (1)$$

$$d = m/Vs \quad (2)$$

where  $Vv$  is the volume of the voids in communication with the surface,  $Vs$  is the total volume, and  $m$  is the mass of the biochar sample. We assessed biochar porosity by firstly drying and then weighing a sample taken from biochar bars. The same sample was then saturated with water and weighed again in order to calculate the overall volume of pores ( $Vv$ ). Then, we soaked the samples in water to calculate the total volume ( $Vs$ ) according to Archimede's principle. We used a high void pump (6 bar) to promote the penetration of water in all open pores. We analyzed samples of cathode material by means of Scanning Electron Microscope (Phenom Pro X), with an integrated Energy-dispersive Detector (EDS) for microanalysis, to identify its elementary composition and to investigate its structure. We performed the analyses before and after using the cathodes in MFCs.

Biochar electrochemical properties were assessed by performing cyclic voltammetry (CVs) before and during MFC operation, with 5 mV/s and at 2 mV/s steps, respectively. We used a sample of 1 cm<sup>2</sup> surface and 0.4 cm thickness as a cathode material to perform preliminary electrode testing. We employed a test solution composed of iron hexacyanoferrate (III) (0.02 M) in a KCl solution (0.1 M) and an Ag/AgCl mini electrode (3.0 M KCl—Biologic©) as the reference electrode. A MiniAutolab Potentiostat (Metrohm©) was used to carry out all electrochemical tests.

### 2.2. MFCs Assembly

In the following, we exploited a single chamber, cuboid MFC made up of acrylic material, able to contain an overall volume of 26 mL of liquid suspension. The anodes were made up of carbon fiber brushes of 25-mm diameter by 35-mm length. The carbon fibers were characterized by a 95% porosity and a 2200 cm<sup>2</sup> total surface for each brush. The brushes were purchased from Mill-Rose ltd. Before using the brushes, the carbon

fibers were activated by soaking them with HCl 0.5M for 8 h and were rinsed at least three times with distilled water. The aim of the treatment was to enrich the surface of the fibers with positive charges, thus facilitating both bacteria adhesion and electroactive biofilm formation [50]. The anode was placed at approximately 3 cm from the cathode inner surface. We fixed biochar slices to one side of the cells by means of screws (Figure 2). The effective cathode surface in contact with the anolyte was 7 cm<sup>2</sup>. We referred to this surface value when we calculated Power Density (PD) and Current Density (CD).

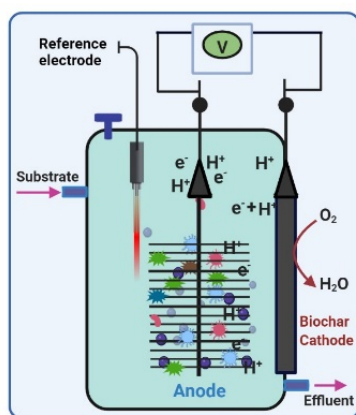


**Figure 2.** MFC filled with shredded organic residues suspension. B: biochar cathode; RE: reference electrode; A: anode.

For electrochemical tests, we placed the Ag/AgCl reference electrode at about 1.5 cm from both cathode and anode surfaces, as shown in Figure 2. During this preliminary research, we did not stir our feedstock.

### 2.3. MFCs Feedstock and Operation

We performed polarization experiments and electric output measurements by using MBED NXP LPC1768 microcontroller and GNU OCTAVE 5.1.0 software. After a starting open circuit voltage (OCV) of 24 h, MFCs were serially connected to a 1000  $\Omega$  resistor for 24 h. After that, we carried out a first polarization experiment (POL) by using a 100,000–100  $\Omega$  range (12 steps) of applied external resistance. Once we had calculated the cell design point, we kept the MFCs at maximum power (MP) for 24 h and then left them in OCV until voltage stabilization before starting a new polarization experiment. We then applied an OCV-POL-MP cycle for the entire duration of the experiment.

We calculated the power and current outputs produced according to Ohm's law. We reported power density (PD) and current density (CD) to the cathode surface in contact with the feedstock (7 cm<sup>2</sup>) and to the mass of solid residues (kg) in the MFC reactors. The feedstock in the MFCs was prepared according to [11] and were modified. Shortly, a sample made up of vegetables (60%), shrubs (15%), fruits (30%), and bread (5%) was suspended and homogenated in phosphate buffer solution 0.1 M (PBS, Applichem). Once prepared, we added glucose (0.5% final concentration) to reduce the start-up phase, as most parts of the organic compounds in vegetable residues are complex molecules like cellulose, lignin, and starch. The resulting slurry was characterized by a 1:3 solid/liquid ratio [5,11,35]. All MFCs were run in duplicate at 25 °C for 15 days, since in our previous experiments we found that the peak performance of MFCs fed with organic substrates occurred within the first two weeks of operation [11]. Overall, we carried out three cycles of measurements for each experimental activity. We performed daily measurements and, as a precaution, adjusted them to  $7.0 \pm 0.2$  by adding KOH (1 M). A *Pseudomonas aeruginosa* ATCC 15692, able to produce both pyochelin and pyocyanine, was purchased from DSMZ strain collection and opportunely cultured in Tryptic Soy Broth (TSB) (Oxoid). After 24 h of incubation at 30 °C, we plated 10  $\mu$ L of suspension on Tryptic Soy Agar (TSA) and incubated it at 37 °C. We prepared 5 mL of microbial suspension in PBS (1 OD<sub>600nm</sub>) using microbial colonies

from a 24-h culture and poured it into MFCs. *P. aeruginosa* final concentration in feedstock was  $10^4$  CFU/mL.

#### 2.4. Effect of *P. aeruginosa* on MFCs Performance

In order to investigate the influence of *P. aeruginosa* activity on MFCs performance, we prepared and monitored three different systems fed with the following substrates and inocula:

- organic residues feedstock
- autoclaved organic residues feedstock + *P. aeruginosa* ATCC 15692
- organic residues feedstock + *P. aeruginosa* ATCC 15692

As to the microflora colonizing the organic residues and electrodes, it was investigated as reported in [11]. We carried out such tests in both MFCs using composite cathode and biochar material. Once we collected PD and CD outputs in polarization experiments of the three systems, we analyzed the data by the *t* Student's and *F* Fisher's tests ( $\sigma = 0.05$ ).

### 3. Results

#### 3.1. Biochar Analyses

The examination of biochar revealed a porosity of 5.1, with a density of  $1.33 \text{ g/cm}^3$ . SEM analyses showed graphite-like structures (Figure 3) composed of carbon (72.4%) and oxygen (23.2%), with a small amount of calcium (2%) and other compounds like sodium (0.8%), silicium (0.4%), and phosphorous (0.8%), Cl (0.4%). The presence of nanophase particles has been detected as well (Figure 3c).

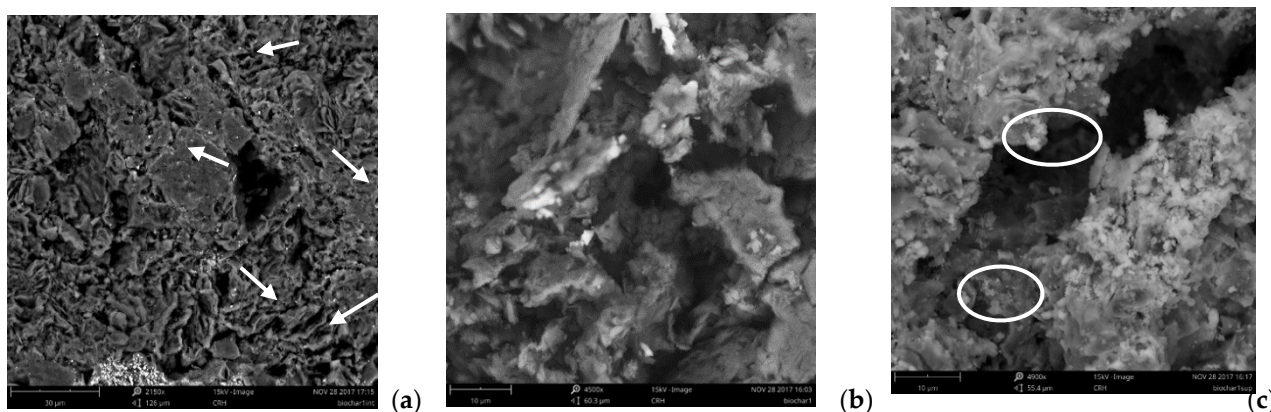


**Figure 3.** Graphite-like structures (white arrows) in biochar section at  $2150\times$  (a),  $4500\times$  (b). (c) Examples of nanophase particles are highlighted by the circles ( $4900\times$ ).

At the end of the experiment, both the inner and outer surfaces of the cathodes showed depositions of a different nature for morphology and composition, as revealed by the microanalysis at the EDS detector (Table 1).

**Table 1.** Elemental composition of biochar and biochar depositions. n.a.: not available \* samples were analyzed after being used in MFCs.

Chemical Elements	Biochar (Clear Zones)	Biochar (Graphite Like Structures)	Inner Surface * (Figure 4a)	Outer Surface * (Figure 4a)
C	51.7	72.1	68.7	64.6
O	33.8	23.3	12.2	5.7
P	4.6	0.8	0.5	n.a.
Ca	5.6	2.0	0.7	n.a.
Na	1.6	0.8	n.a.	18.9
Cl	0.4	0.4	1.0	10.9
Si	0.5	0.4	0.4	n.a.
Mg	1.4	n.a.	n.a.	n.a.
Mo	n.a.	n.a.	0.2	n.a.
K	0.4	n.a.	n.a.	n.a.
Fe	n.a.	n.a.	9.4	n.a.
Zn	n.a.	n.a.	6.5	n.a.
In	n.a.	n.a.	0.3	n.a.

It is interesting to notice that the depositions at the outer side of the cathode (Figure 4b) were composed mainly of NaCl, which was present in the feedstock suspension used to fuel the MFCs. On the other hand, the depositions on the inner side can be ascribed to the microbial activity (biofilm on the cathode) and to the presence of organic particles in the medium, the NaCl present on the surface exposed to the air can be explained with the biochar behaviour as semipermeable material, thanks to the presence of charged groups.

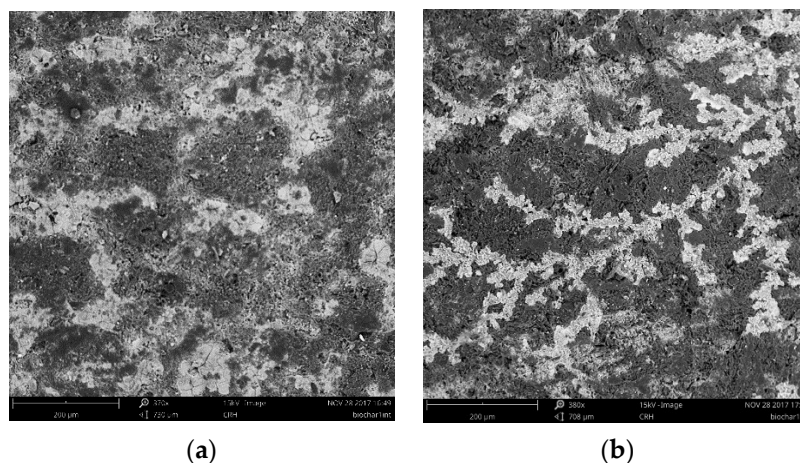


**Figure 4.** Inner (a) and outer (b) cathode surfaces at 370 $\times$  and 380 $\times$  magnification. The arrows in (a) mark residues that can be ascribed to biofilm growth while in (b) arrows indicate salts (mainly NaCl) depositions.

CV carried out with iron hexacyanoferrate (III) solution 0.02M revealed two reduction peaks due to negative currents at +170 mV and +387 mV and an oxidation peak at +570 mV (Figure 5). If the +570 and +170 mV peaks could be ascribed to the oxidation and reduction of Fe in solution, the nature of the third one at +387 mV as well as the cross-over potentials ( $E_{x1}$  and  $E_{x2}$ ) should still be investigated. Crossover potentials between the cathodic and anodic current traces can occur in consequence of a difference in deposition and dissolution potentials at a specific potential value. Hence, the presence of the cross-

over is diagnostic for nuclei formation (electrodeposition) on the electrode [51]. Multiple cross-over points may be ascribed to nucleation mechanisms involving complex chemical reactions among the redox species in the bulk ( $\text{Fe}^{2+}/\text{Fe}^{3+}$ , in this case) and metals or other complexes on the electrode surface. As shown in Table 1, the microanalysis with EDS detector revealed, among other things, the presence of zinc, molybdenum, iron and indium. Nevertheless, there is a need for further analyses to better characterize biochar composition and electrochemical behavior.

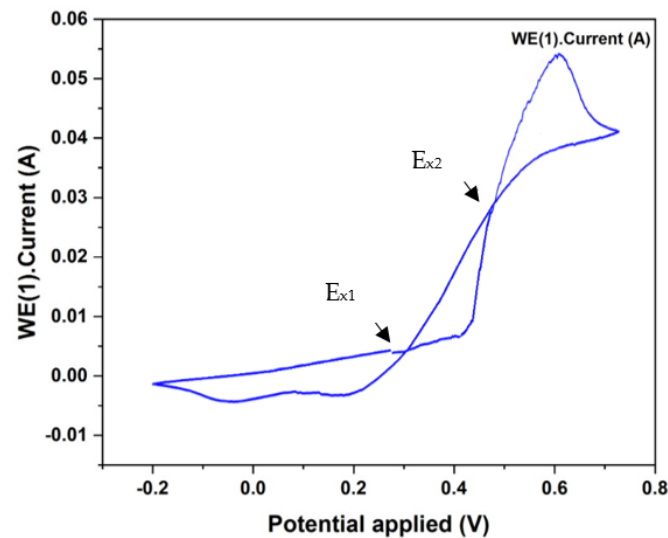


**Figure 5.** Biochar CV (5 mV/s) in iron hexacyanoferrate (III) 0.02M, 0.1 M KCl. The arrows indicate the two crossing points ( $E_{x1}$  and  $E_{x2}$ ).

( $E_{x1}$  and  $E_{x2}$ ) When used as a cathode in MFCs, biochar slices gave the results reported in Figure 6, where a CV at 2 mV/s speed and performed at a +1 V/−1 V range is reported. Our results show that the cathodic current (−0.0058 A) is prevalent in comparison to the anodic one (+0.00045 A), thus confirming the proper behaviour as a cathode in MFCs. The absence of reduction/oxidation peaks indicates the direct electron transfer mechanisms, which is very likely mediated by bacteria colonizing the cathode itself. Nevertheless, a significant overpotential limited the cathode performance (Cathode OCP vs. Ag/AgCl reference electrode =  $-0.214 \pm 0.02$  V). A cross-over point was detected at −260 mV, whose meaning will be further investigated.

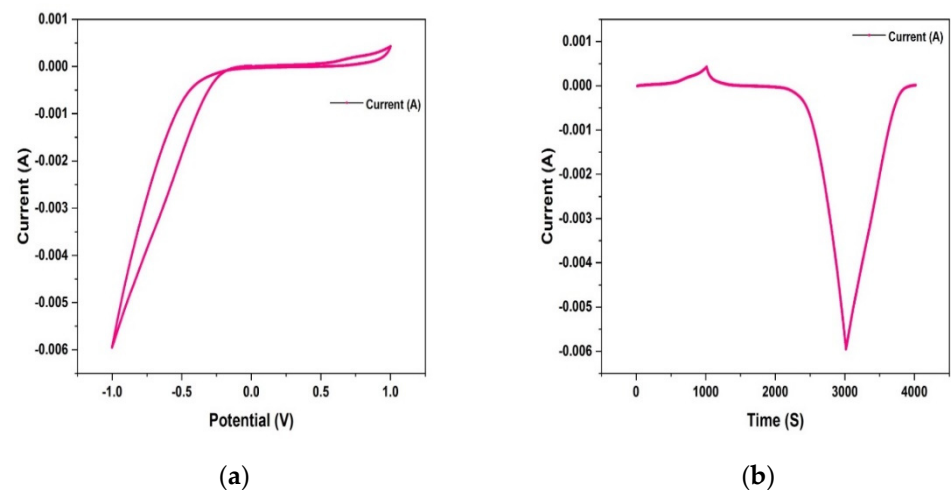


**Figure 6.** Current peaks over time (a) and cyclic voltammogram (b) of biochar cathode during MFC operation.



### 3.2. Polarization Behaviour

In Figure 7, we report the power and polarization curves based on voltage, current and power average values collected during polarization experiments carried out every 48 h for two weeks during three independent experiments. PD and CD values refer to the cathode surfaces and the amount of solid residues (Figure 7). Even though P\_MFCs had higher power outputs, we observed a progressive reduction in their performance after the first week of utilization. P\_MFCs and B\_FCs showed a cell design point of  $1200 \Omega$  and  $8000 \Omega$  respectively. B-MFC outputs were, on average,  $0.19 \text{ Wm}^{-2}\text{kg}^{-1}$  and  $7.5 \text{ Am}^{-2}\text{kg}^{-1}$ , with peaks of 0.32 and  $35.6 \text{ Am}^{-2}\text{kg}^{-1}$ . As to P\_MFCs, the average PD and CD values were  $2.67 \text{ Wm}^{-2} \text{ kg}^{-1}$  and  $7.5 \text{ Am}^{-2}\text{kg}^{-1}$ , with peaks of  $4.87 \text{ Wm}^{-2}\text{kg}^{-1}$  and  $35.6 \text{ Am}^{-2} \text{ kg}^{-1}$ .

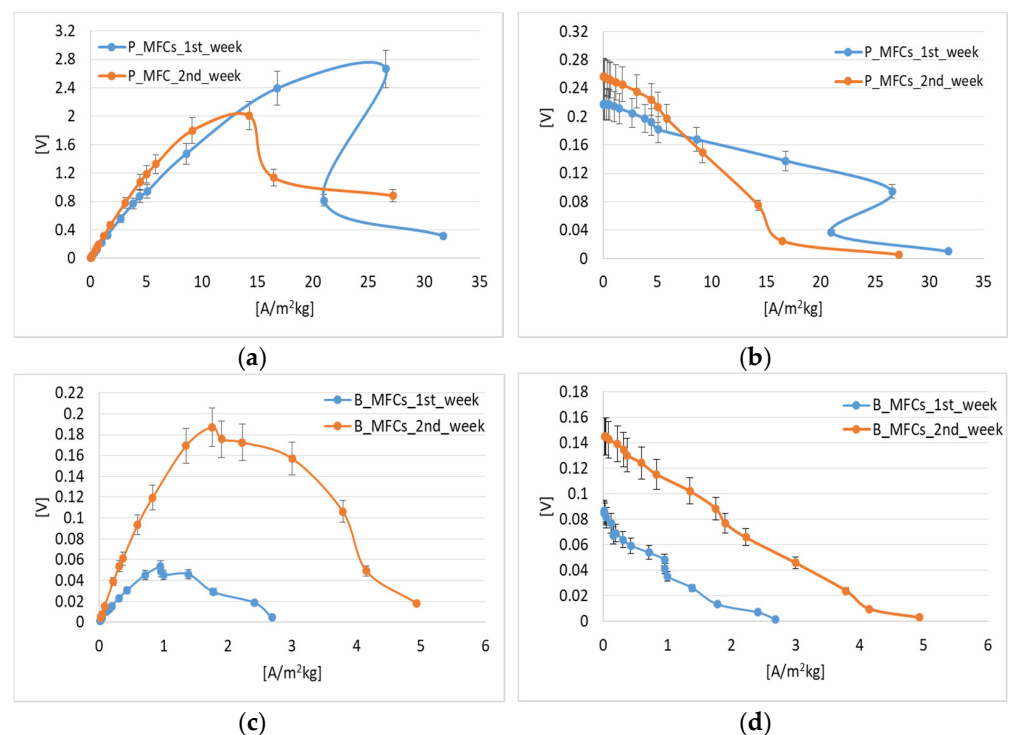


**Figure 7.** P\_MFCs (a,b) and B-MFC (c,d) power and polarization curves. The diagrams report voltage, current and power densities average values  $\pm$ SE over three independent experiments.

An overshoot characterised the polarization behaviour of P\_MFCs during the second week of operation. Such a behaviour can be ascribed to concentration losses, leading to a dramatic decrease in both current and power, unlike what was observed in B\_MFCs, whose cathode material, which kept its properties even after being used in three different experiments (Figure 7). At last, P\_MFC underwent a voltage reversal due to electrode fouling. As to pH, we measured a drop from 7.0 to 4.5 in P\_MFC after two days of operation, while in B-MFC, pH values did not significantly deviate from  $6.6 \pm 0.3$  along with the experiment. After dropping to 4.5, pH in P\_MFC was adequately corrected to  $7.0 \pm 0.2$  and was kept around that value by using KOH 1M. As to OCV, in Figure 8, we report that the OCV values measured during five cycle of measurement in P\_MFCs and B\_MFCs were fed with only organic residues (thus in presence of the sole endogenous microflora) as an example of the behaviour of both systems along with the experiment. As expected, the addition of a fresh substrate (5 mL) increased the voltage of both systems due to the increase in fermentative metabolism.

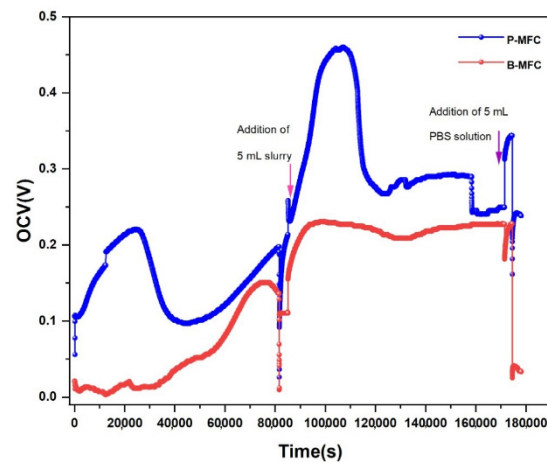


**Figure 8.** OCV values during five OCV\_POL\_PMax (P\_MFCs and B\_MFCs). The arrows indicate the addition of substrate (slurry) and PBS solution.

### 3.3. Influence of *Pseudomonas aeruginosa* on MFC Performance

The microbial microflora in vegetable waste was mainly composed of *Lactobacillus*, *Bacillus*, and *Clostridium* strains [11], the main components of acidophilic and acidogenic microflora. *P. aeruginosa* ATCC 15,692 was able to use the substrate from both autoclaved and non-autoclaved organic residues as a source of carbon and energy with higher outputs in comparison to the endogenous microflora. Better results were achieved when *P. aeruginosa* ATCC 15,692 was inoculated in raw organic waste and were thus in presence of microorganisms already present in the waste. Microbiological analyses with culture media showed the growth of *P. aeruginosa* at the cathode with a density of 1.5 CFU/cm<sup>2</sup>, while no growth was detected at the anode. The absence of *P. aeruginosa* at the anode can find a suitable explanation in its aerobic/anoxic metabolism: this microorganism can find more suitable conditions for its growth at the cathode.

The increase in electron transfer in MFCs with mixed cultures is supported by the significant improvement of CD: from 16.2 Am<sup>-2</sup>kg<sup>-1</sup> of the sole endogenous microflora, to 32.9 Am<sup>-2</sup>kg<sup>-1</sup> of *P. aeruginosa* and 67 Am<sup>-2</sup>kg<sup>-1</sup> of the endogenous bacteria + *P. aeruginosa*. Even when inoculated in B-MFCs, we observed a significant increase in current and power outputs (Figure 9).

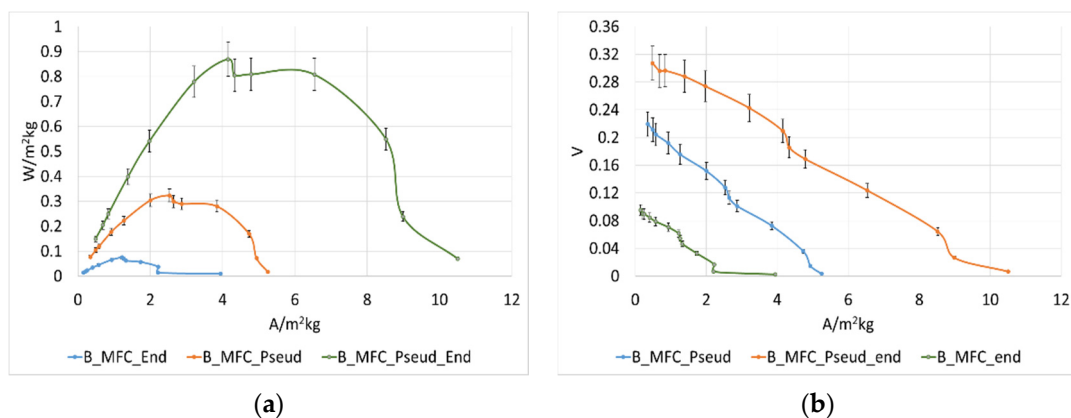


**Figure 9.** Cont.

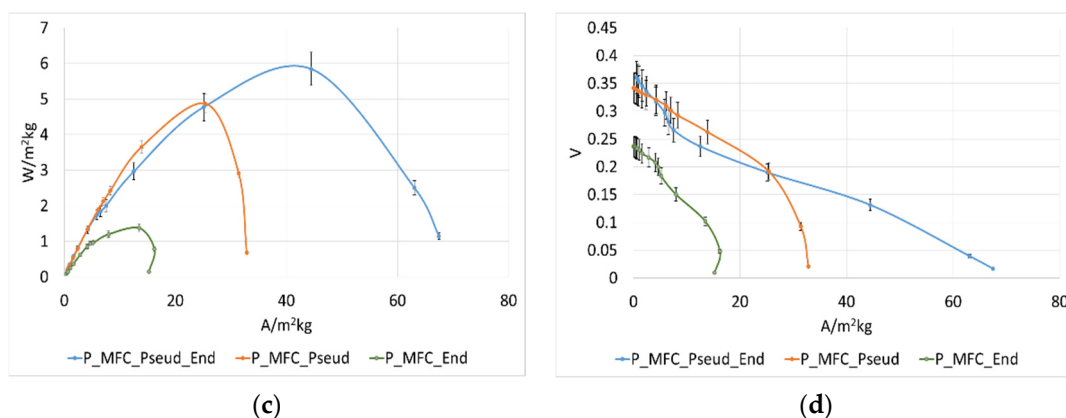


**Figure 9.** Power and polarization curves in B\_MFCs (a,b) and P\_MFCs (c,d) in the presence of *P. aeruginosa* + endogenous microflora (End\_Pseud); *P. aeruginosa* (Pseud) and endogenous microflora (End). The diagrams report the average values  $\pm$ SE over three independent experiments.

As to PD, it increased from the  $1.4 \text{ W m}^{-2} \text{ kg}^{-1}$  of the sole acidogenic bacteria to  $5.8 \text{ W m}^{-2} \text{ kg}^{-1}$  achieved when *P. aeruginosa* was added to the resident microflora. A similar pattern was observed by some of the authors of this paper in previous MFCs (1 L in volume) provided with graphite plates with a gas diffusion layer (GDL) as air-breathing cathodes and using organic residues as feedstock [5,35]. When *P. aeruginosa* was present at the cathode of such MFCs, we detected the presence of both oxidation and reduction peaks, as shown in Figure 10. Such peaks were absent at the anode, where just a Gram-positive microflora was present (see [11] for further details). This outcome can be explained by the use of phenazines as electron shuttles and by other microorganisms (Gram-positive bacteria, *Enterobacteriaceae*, etc.) besides *P. aeruginosa*. The shared utilization of phenazines by a mixed microbial population led to an increase in both current and power production [41]. Our hypothesis was confirmed by the production of phenazines, assessed by the culture of was the *P. aeruginosa* previously isolated at the cathode on Kings' A and B media for the detection of pyocyanin and pyoverdine [11].

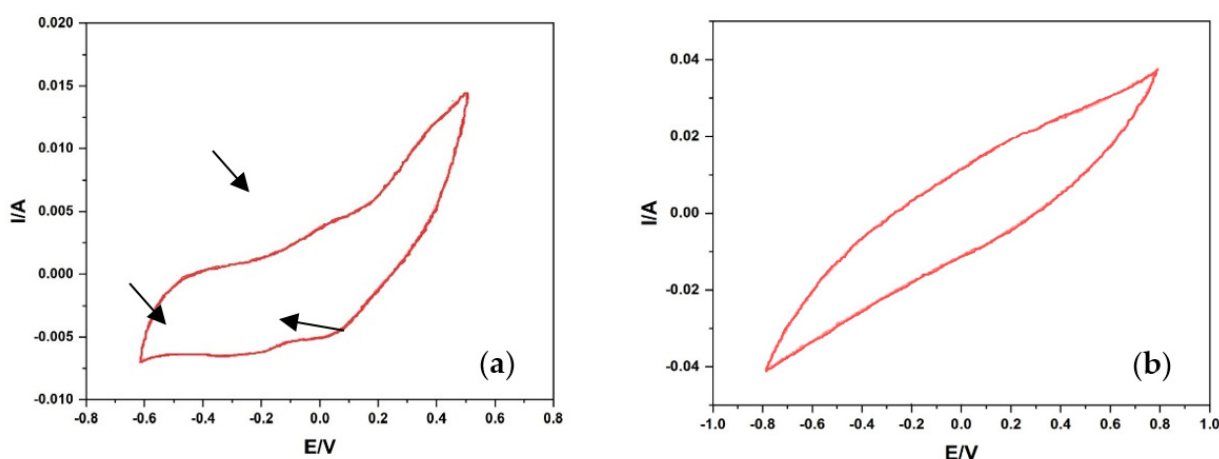


**Figure 10.** CV (Ag/AgCl) reference of cathode (a) and anode (b) of a MFC fed with organic residues and in which *P. aeruginosa* was present at the cathode [11]. Reduction peaks at  $-0.280 \text{ V}$  and  $+0.070 \text{ V}$  and an oxidation peak at  $+0.120 \text{ V}$  at  $\text{pH } 7.0 \pm 0.2$ .

Statistical analyses of the data collected from biochar MFCs with different inocula showed significant differences at *t* test in terms of PD when we compare the outputs of MFCs inoculated with no sterile substrate in the presence and absence of *P. aeruginosa*, with  $p \sim 0.0001$  for the *t* test and a  $p < 0.0001$  for the *F* test. Even when inoculated in a

sterile substrate, *P. aeruginosa* gave a higher PD in comparison to the endogenous bacteria (Table 2).

**Table 2.** Statistical analyses results. \* indicates  $p < 0.05$ .

	Pseud_End/End	Pseud_End/Pseud	Pseud/End
	Test t	Test t	Test t
CD	0.119	0.316	0.417
PD	0.0001 *	0.131	0.0218 *
	Test F	Test F	Test F
CD	0.0001 *	0.022 *	0.063
PD	$2.59 \times 10^{-1}$ *	0.736	$4.97 \times 10^{-10}$ *

#### 4. Conclusions

As a scrap substrate, biochar is very cheap and, due to its properties, it was able to sustain SMFC operation using organic residues as a source of energy and with an acidogenic microflora as its main component. Even though MFCs with a biochar cathode achieved less PD and CD in comparison to the composite, the possibility to use it for more than one cycle and, then to recycle the cathode itself as a soil fertility improver represents an advantage in comparison to more complex and expensive materials like nickel-mesh-activated-carbon and PTFE-layer electrodes. Nevertheless, the structure and electrochemical properties of biochar material need to be better investigated in order to optimize its utilization at the cathode. Parallel to these experimental activities, advanced numerical methods will be developed to predict the performance of MFCs, leveraging both the boost in computational power and the recent results achieved in biophysical complex system simulation [52,53]. The abundance of fermentative bacteria in vegetable residues can limit the performances of MFC applications to solid waste treatment and valorization. Our results suggest that an improvement in the MFC performances could be achieved by enriching the biomass with an attenuated *Pseudomonas aeruginosa* strain or by adding molecules (better if from natural sources) acting as electron shuttles to increase the electrons flow to the electrodes.

**Author Contributions:** Conceptualization, G.F.; methodology, supervision, validation and funding acquisition R.A.N.; investigation and data curation F.F., E.G., N.S.; visualization and formal analysis, K.C.; Writing—original draft, R.A.N. and K.C.; Writing—review and editing, G.F. and K.C. All authors have read and agreed to the published version of the manuscript.

**Funding:** En.Tech Italia srl provided fundings for this research.

**Institutional Review Board Statement:** Not applicable.

**Informed Consent Statement:** Not applicable.

**Data Availability Statement:** Not applicable.

**Conflicts of Interest:** The authors declare no conflict of interest.

#### References

1. Endreny, T.; Avignone-Rossa, C.; Nastro, R.A. Generating electricity with urban green infrastructure microbial fuel cells. *J. Clean. Prod.* **2020**, *263*, 121337. [[CrossRef](#)]
2. Chandrasekhar, K.; Kadier, A.; Kumar, G.; Nastro, R.A.; Jeevitha, V. Challenges in Microbial Fuel Cells and Future Scope. In *Microbial Fuel Cell: A Bioelectrochemical System That Convert Waste into Watts*; Capital/Publishing Company: New Delhi, India; Springer: Cham, Switzerland, 2017.
3. Nastro, R.A.; Falcucci, G.; Minutillo, M.; Jannelli, E. Microbial Fuel Cells in Solid Waste Valorization: Trends and Applications. In *Recent Trends in Management of Solid and Hazardous Waste*; Springer Nature: Cham, Switzerland, 2016.
4. Winfield, J.; Gajda, I.; Greenman, J.; Ieropoulos, I. A review into the use of ceramics in microbial fuel cells. *Bioresour. Technol.* **2016**, *215*, 296–303. [[CrossRef](#)] [[PubMed](#)]

5. Jannelli, N.; Nastro, R.A.; Cigolotti, V.; Minutillo, M.; Falcucci, G. Low pH, high salinity: Too much for microbial fuel cells? *Appl. Energy* **2017**, *192*, 543–550. [[CrossRef](#)]
6. Khan, M.D.; Khan, N.; Sultana, S.; Joshi, R.; Ahmed, S.; Yu, E.; Scott, K.; Ahmad, A.; Khan, M.Z. Bioelectrochemical conversion of waste to energy using microbial fuel cell technology. *Process. Biochem.* **2017**, *57*, 141–158. [[CrossRef](#)]
7. Ahmad, J.; Patuzzi, F.; Rashid, U.; Shahabz, M.; Ngamcharussrivichai, C.; Baratieri, M. Exploring untapped effect of process conditions on biochar characteristics and applications. *Environ. Technol. Innov.* **2021**, *21*, 101310. [[CrossRef](#)]
8. Gambino, E.; Toscanesi, M.; Del Prete, F.; Flagiello, F.; Falcucci, G.; Minutillo, M.; Trifuoggi, M.; Guida, M.; Nastro, R.A.; Jannelli, E. Polycyclic aromatic hydrocarbons (PAHs) degradation and detoxification of water environment in single-chamber air-cathode microbial fuel cells (MFCs). *Fuel Cells* **2017**, *17*, 618–626. [[CrossRef](#)]
9. Di Ilio, G.; Falcucci, G. Multiscale methodology for microbial fuel cell performance analysis. *Int. J. Hydrogen Energy* **2021**, *46*, 20280–20290. [[CrossRef](#)]
10. Chandrasekhar, K.; Kumar, A.N.; Kumar, G.; Kim, D.H.; Song, Y.C.; Kim, S.H. Electro-fermentation for biofuels and biochemicals production: Current status and future directions. *Bioresour. Technol.* **2021**, *323*, 124598. [[CrossRef](#)]
11. Florio, C.; Nastro, R.A.; Flagiello, F.; Minutillo, M.; Pirozzi, D.; Pasquale, V.; Ausiello, A.; Toscano, G.; Jannelli, E.; Dumontet, S. Biohydrogen production from solid phase-microbial fuel cell spent substrate: A preliminary study. *J. Clean. Prod.* **2019**, *227*, 506–511. [[CrossRef](#)]
12. Kumar, P.; Chandrasekhar, K.; Kumari, A.; Sathiyamoorthi, E.; Kim, B.S. Electro-fermentation in aid of bioenergy and biopolymers. *Energies* **2018**, *11*, 343. [[CrossRef](#)]
13. Schievano, A.; Pant, D.; Puig, S. Microbial synthesis, gas-fermentation and bioelectroconversion of CO<sub>2</sub> and other gaseous streams. *Front. Energy Res.* **2019**, *7*, 110. [[CrossRef](#)]
14. Sasaki, K.; Sasaki, D.; Tsuge, Y.; Morita, M.; Kondo, A. Enhanced methane production from cellulose using a two-stage process involving a bioelectrochemical system and a fixed film reactor. *Biotechnol. Biofuels* **2021**, *14*, 7. [[CrossRef](#)]
15. Im, C.H.; Kim, C.; Song, Y.E.; Oh, S.E.; Jeon, B.H.; Kim, J.R. Electrochemically enhanced microbial CO conversion to volatile fatty acids using neutral red as an electron mediator. *Chemosphere* **2018**, *191*, 166–173. [[CrossRef](#)] [[PubMed](#)]
16. Li, H.; Tian, Y.; Zuo, W.; Zhang, J.; Pan, X.; Li, L.; Su, X. Electricity generation from food wastes and characteristics of organic matters in microbial fuel cell. *Bioresour. Technol.* **2016**, *205*, 104–110. [[CrossRef](#)] [[PubMed](#)]
17. Rabaey, K.; Rozendal, R. Microbial electrosynthesis—Revisiting the electrical route for microbial production. *Nat. Rev. Microbiol.* **2010**, *8*, 706–716. [[CrossRef](#)] [[PubMed](#)]
18. Sivagurunathan, P.; Kuppam, C.; Mudhoo, A.; Saratale, G.D.; Kadier, A.; Zhen, G.; Chatellard, L.; Trably, E.; Kumar, G. A comprehensive review on two-stage integrative schemes for the valorization of dark fermentative effluents. *Crit. Rev. Biotechnol.* **2018**, *38*, 868–882. [[CrossRef](#)] [[PubMed](#)]
19. Nastro, R.A.; Leccisi, E.; Toscanesi, M.; Liu, G.; Trifuoggi, M.; Ulgiati, S. Exploring avoided environmental impacts as well as energy and resource recovery from microbial desalination cell treatment of brine. *Energies* **2021**, *14*, 4453. [[CrossRef](#)]
20. Flagiello, F.; Gambino, E.; Nastro, R.A.; Chandrasekhar, K. Harvesting Energy Using Compost as a Source of Carbon and Electrogenic Bacteria. In *Bioelectrochemical Systems*; Springer Nature: Cham, Switzerland, 2020.
21. Jung, S.; Lee, J.; Park, Y.K.; Kwon, E.E. Bioelectrochemical systems for a circular bioeconomy. *Bioresour. Technol.* **2020**, *300*, 122748. [[CrossRef](#)] [[PubMed](#)]
22. Senthilkumar, K.; Naveenkumar, M. Enhanced performance study of microbial fuel cell using waste biomass-derived carbon electrode. *Biomass Conv. Bioref.* **2021**, 1–9. [[CrossRef](#)]
23. Rahman, M.Z.; Edvinsson, T.; Kwong, P. Biochar for electrochemical applications. *Curr. Opin. Green Sustain. Chem.* **2020**, *23*, 25–30. [[CrossRef](#)]
24. Zha, Z.; Zhang, Z.; Xiang, P.; Zhu, H.; Zhou, B.; Sun, Z.; Zhou, S. One-step preparation of eggplant-derived hierarchical porous graphitic biochar as efficient oxygen reduction catalyst in microbial fuel cells. *RSC Adv.* **2021**, *11*, 1077–1085. [[CrossRef](#)]
25. Li, S.; Ho, S.H.; Hua, T.; Zhou, Q.; Li, F.; Tang, J. Sustainable biochar as an electrocatalysts for the oxygen reduction reaction in microbial fuel cells. *Green Energy Environ.* **2020**. [[CrossRef](#)]
26. Minutillo, M.; Flagiello, F.; Nastro, R.A.; Di Trollo, P.; Jannelli, E.; Perna, A. Performance of two different types of cathodes in microbial fuel cells for power generation from renewable sources. *Energy Procedia* **2018**, *148*, 1129–1134. [[CrossRef](#)]
27. Chakraborty, I.; Sathe, S.M.; Dubey, B.K.; Ghangrekar, M.M. Waste-derived biochar: Applications and future perspective in microbial fuel cells. *Bioresour. Technol.* **2020**, *312*, 123587. [[CrossRef](#)] [[PubMed](#)]
28. Joseph, S.; Husson, O.; Graber, E.R.; van Zwieten, L.; Taherymoosavi, S.; Thomas, T.; Nielsen, S.; Ye, J.; Pan, G.; Chia, C.; et al. The electrochemical properties of biochars and how they affect soil redox properties and processes. *Agronomy* **2015**, *5*, 322. [[CrossRef](#)]
29. Wang, J.; Song, X.; Li, Q.; Bai, H.; Zhu, C.; Weng, B.; Yan, D.; Bai, J. Bioenergy generation and degradation pathway of phenanthrene and anthracene in a constructed wetland-microbial fuel cell with an anode amended with nZVI. *Water Res.* **2019**, *150*, 340–348. [[CrossRef](#)]
30. Mian, M.; Liu, G.; Fu, B. Conversion of sewage sludge into environmental catalyst and microbial fuel cell electrode material: A review. *Sci. Total Environ.* **2019**, *666*, 525–539. [[CrossRef](#)] [[PubMed](#)]
31. Cheng, D.; Ngo, H.H.; Guo, W.; Chang, W.S.; Nguyen, D.D.; Li, J.; Ly, Q.V.; Nguyen, T.A.H.; Tran, V.S. Applying a new pomelo peel derived biochar in microbial fuel cell for enhancing sulfonamide antibiotics removal in swine wastewater. *Bioresour. Technol.* **2020**, *318*, 123886. [[CrossRef](#)]

32. Huggins, T.M.; Latorre, A.; Biffinger, J.C.; Ren, Z.J. Biochar based microbial fuel cell for enhanced wastewater treatment and nutrient recovery. *Sustainability* **2016**, *8*, 169. [[CrossRef](#)]
33. Ayyappan, C.S.; Bhalambaal, V.M.; Kumar, S. Effect of biochar on bio-electrochemical dye degradation and energy production. *Bioresour. Technol.* **2018**, *251*, 165–170. [[CrossRef](#)]
34. Ganesh, K.; Jambeck, J.R. Treatment of landfill leachate using microbial fuel cells: Alternative anodes and semi-continuous operation. *Bioresour. Technol.* **2013**, *139*, 383–387. [[CrossRef](#)] [[PubMed](#)]
35. Nastro, R.A.; Falcucci, G.; Toscanesi, M.; Minutillo, M.; Pasquale, V.; Trifuoggi, M.; Dumontet, S.; Jannelli, E. Performances and Microbiology of a Microbial Fuel Cell (MFC) Fed with the Organic Fraction of Municipal Solid Waste (OFMSW). In Proceedings of the EFC2015 European Fuel Cell Technology & Applications Conference—Piero Lunghi Conference, Naples, Italy, 15–18 December 2015.
36. Chandrasekhar, K.; Amulya, K.; Venkata Mohan, S. Solid phase bio-electrofermentation of food waste to harvest value-added products associated with waste remediation. *Waste Manag.* **2015**, *45*, 57–65. [[CrossRef](#)]
37. Budihardjo, M.A.; Effendi, A.J.; Hidayat, S.; Purnawan, C.; Lantasi, A.I.D.; Muhammad, F.I.; Ramadan, B.S. Waste valorization using solid-phase microbial fuel cells (SMFCs): Recent trends and status. *J. Environ. Manag.* **2021**, *277*, 111417. [[CrossRef](#)] [[PubMed](#)]
38. Wang, H.; Luo, H.; Fallgren, P.H.; Jin, S. Bioelectrochemical system platform for sustainable environmental remediation and energy generation. *Biotechnol. Adv.* **2015**, *33*, 317–334. [[CrossRef](#)]
39. Di Ilio, G.; Nastro, R.A.; Di Trolio, P.; Falcucci, G. A Comprehensive Multiscale Methodology to Investigate Microbial Fuel Cell Performance. In Proceedings of the ECOS 2019—32nd International Conference on Efficiency, Cost, Optimization, Simulation and Environmental Impact of Energy Systems, Wroclaw, Poland, 23–28 June 2019; pp. 3841–3857.
40. Zheng, T.; Li, J.; Ji, Y.; Zhang, W.; Fang, Y.; Xin, F.; Dong, W.; Wei, P.; Ma, J.J.M. Progress and prospects of bioelectrochemical systems: Electron transfer and its applications in the microbial metabolism. *Front. Bioeng. Biotechnol.* **2020**, *8*, 10. [[CrossRef](#)]
41. Rabaey, K.; Boon, N.; Höfte, M.; Verstraete, W. Microbial phenazine production enhances electron transfer in biofuel cells. *Environ. Sci. Technol.* **2005**, *39*, 3401–3408. [[CrossRef](#)] [[PubMed](#)]
42. Qiao, Y.J.; Qiao, Y.; Zou, L.; Wu, X.S.; Liu, J.H. Biofilm promoted current generation of *Pseudomonas aeruginosa* microbial fuel cell via improving the interfacial redox reaction of phenazines. *Bioelectrochemistry* **2017**, *117*, 34–39. [[CrossRef](#)]
43. Pham, H.T.; Boon, N.; De Maeyer, K.; Höfte, M.; Rabaey, K.; Verstraete, W. Use of *Pseudomonas* species producing phenazine-based metabolites in the anodes of microbial fuel cells to improve electricity generation. *Appl. Microbiol. Biotechnol.* **2008**, *80*, 985–993. [[CrossRef](#)] [[PubMed](#)]
44. Marone, A.; Izzo, G.; Mentuccia, L.; Massini, G.; Paganin, P.; Rosa, S.; Varrone, C.; Signorini, A. Vegetable waste as substrate and source of suitable microflora for bio-hydrogen production. *Renew. Energy* **2014**, *68*, 6–13. [[CrossRef](#)]
45. Panin, S.; Setthapun, W.; Sinsuw, A.A.E.; Sintuya, H.; Chu, C.Y. Biohydrogen and biogas production from mashed and powdered vegetable residues by an enriched microflora in dark fermentation. *Int. J. Hydrogen Energy* **2021**, *46*, 14073–14082. [[CrossRef](#)]
46. Paquete, C.M. Electroactivity across the cell wall of gram-positive bacteria. *Comput. Struct. Biotechnol. J.* **2020**, *18*, 3796–3802. [[CrossRef](#)]
47. Brooijmans, R.J.W.; de Vos, W.M.; Hugenholtz, J. *Lactobacillus plantarum* WCFS1 electron transport chains. *Appl. Environ. Microbiol.* **2009**, *75*, 3580–3585. [[CrossRef](#)] [[PubMed](#)]
48. Tomczyk, A.; Sokołowska, Z.; Boguta, P. Biochar physicochemical properties: Pyrolysis temperature and feedstock kind effects. *Rev. Environ. Sci. Biotechnol.* **2020**, *19*, 191–215. [[CrossRef](#)]
49. Zhang, Y.; Xu, X.; Cao, L.; Ok, Y.S.; Cao, X. Characterization and quantification of electron donating capacity and its structure dependence in biochar derived from three waste biomasses. *Chemosphere* **2018**, *211*, 1073–1081. [[CrossRef](#)] [[PubMed](#)]
50. Yaqoob, A.A.; Mohamad, I.M.N.; Rafatullah, M.; Chua, Y.S.; Ahmad, A.; Umar, K. Recent advances in anodes for microbial fuel cells: An overview. *Materials* **2020**, *13*, 2078. [[CrossRef](#)] [[PubMed](#)]
51. Mallik, A.; Ray, B.C. Evolution of principle and practice of electrodeposited thin film: A review on effect of temperature and sonication. *Int. J. Electrochem.* **2011**, *2011*, 16. [[CrossRef](#)]
52. Falcucci, G.; Amati, G.; Fanelli, P.; Krastev, V.K.; Polverino, G.; Porfiri, M.; Succi, S. Extreme flow simulations reveal skeletal adaptations of deep-sea sponges. *Nature* **2021**, *595*, 537–541. [[CrossRef](#)]
53. Krastev, V.K.; Falcucci, G. Evaluating the electrochemical and power performances of microbial fuel cells across physical scales: A novel numerical approach. *Int. J. Hydrogen Energy* **2019**, *44*, 4468–4475. [[CrossRef](#)]